Magnetic Diagnostics for Plasmas

Tokamak Engineering and Operation

Outline

Outline

Portuguese Discoveries, XV - XVI Centuries

The Portuguese Heroes

Henry the Navigator 1394-1460

King John II 1455-1495

Vasco da Gama 1460-1524

Pedro Alvares Cabral 1467-1520

Ferdinand Magellan 1480 1521

The Instruments

The Caravel

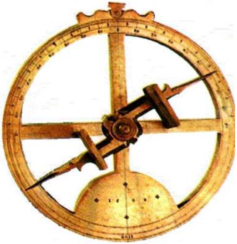

The Astrolabe

The Instruments

The Caravel

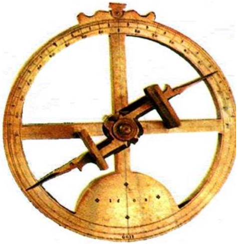

The Astrolabe

The Compass

Magnetic Diagnostics in Fusion: General Principles

Magnetic measurements provide some of the most fundamental and essential information about a fusion plasma:

- I_{plasma}, Internal Inductance ℓ_i, Position and Speed of current centroid, Boundary Shape, Thermal Energy, Currents in the magnet coils, and the strength of the magnetic fields confining the plasma.
- Information about the internal characteristics of the plasma and about asymmetries caused by large-scale MHD instabilities.
- Halo Currents in machine structures.

Magnetic Diagnostics in Fusion: General Principles

Magnetic measurements provide some of the most fundamental and essential information about a fusion plasma:

- I_{plasma}, Internal Inductance ℓ_i, Position and Speed of current centroid, Boundary Shape, Thermal Energy, Currents in the magnet coils, and the strength of the magnetic fields confining the plasma.
- Information about the internal characteristics of the plasma and about asymmetries caused by large-scale MHD instabilities.
- Halo Currents in machine structures.

Magnetic Diagnostics in Fusion: General Principles

Magnetic measurements provide some of the most fundamental and essential information about a fusion plasma:

- I_{plasma}, Internal Inductance ℓ_i, Position and Speed of current centroid, Boundary Shape, Thermal Energy, Currents in the magnet coils, and the strength of the magnetic fields confining the plasma.
- Information about the internal characteristics of the plasma and about asymmetries caused by large-scale MHD instabilities.
- Halo Currents in machine structures.

TÉCNICO LISBOA

Magnetic Diagnostics in Fusion: General Principles

Magnetic measurements provide some of the most fundamental and essential information about a fusion plasma:

- I_{plasma}, Internal Inductance ℓ_i, Position and Speed of current centroid, Boundary Shape, Thermal Energy, Currents in the magnet coils, and the strength of the magnetic fields confining the plasma.
- Information about the internal characteristics of the plasma and about asymmetries caused by large-scale MHD instabilities.
- Halo Currents in machine structures.

General Principles II

- Essential for Equilibrium Reconstructions
  - Post-discharge full equilibrium codes
  - Real-Time Plasma Shape and Position Control
- Magnetic diagnostics are external, passive and ROBUST!
  - The measurements remain valid and useful over the full range of plasma density and temperature as well as during large transient events (disruptions).

General Principles II

- Essential for Equilibrium Reconstructions
  - Post-discharge full equilibrium codes
  - Real-Time Plasma Shape and Position Control
- Magnetic diagnostics are external, passive and ROBUST!
  - The measurements remain valid and useful over the full range of plasma density and temperature as well as during large transient events (disruptions).

Axisymmetric Configuration of Fusion Devices

Magnetic field

- In a cylindrical coordinate system, (R, Z, ϕ), $\vec{B}$ can be expressed in terms of two scalar functions, F, and Ψ:

$$\vec{B} = (F\,\hat{\phi} + \nabla\Psi \times \hat{\phi})/R$$

- $\vec{B}$ field can be separated in
  - Toroidal Field: $\vec{B}_\phi = \frac{F}{R}\,\hat{\phi}$
  - Poloidal Field: $\vec{B}_p = \frac{\nabla\Psi}{R}$

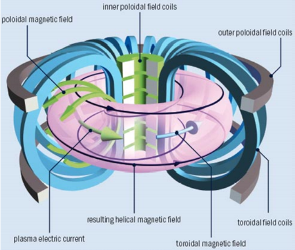

Axisymmetric Configuration of Fusion Devices

Magnetic field

- In a cylindrical coordinate system, (R, Z, ϕ), $\vec{B}$ can be expressed in terms of two scalar functions, F, and Ψ:

$$\vec{B} = (F\,\hat{\phi} + \nabla\Psi \times \hat{\phi})/R$$

- $\vec{B}$ field can be separated in
  - Toroidal Field: $\vec{B}_\phi = \frac{F}{R}\,\hat{\phi}$
  - Poloidal Field: $\vec{B}_p = \frac{\nabla\Psi}{R}$

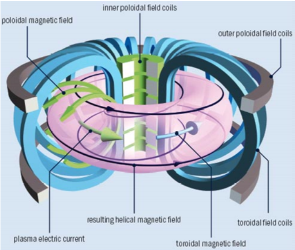

Axisymmetric Configuration

Poloidal Fluxes

Magnetic Flux

Mag. Poloidal flux (PF), $\Psi(R,Z)$ over one major circle, at (R,Z).

$$\psi(R,Z) = \frac{\Psi(R,Z)}{2\pi}, \text{ flux per radian}$$
$$\Psi(R,Z) = \iint d\vec{B}\cdot d\vec{S}$$

Current Flux

Poloidal current function, F, crossing the major circle, at (R,Z).

$$F(R,Z) = \mu I_{pol}\Psi(R,Z)/2\pi = R\,B_\phi$$
$$I_{pol}(R,Z) = \iint d\vec{j}_{pol}\cdot d\vec{S}$$

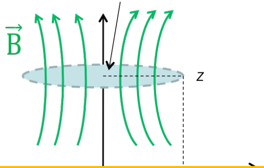

Axisymmetric Configuration

Poloidal Fluxes

Magnetic Flux

Mag. Poloidal flux (PF), $\Psi(R,Z)$ over one major circle, at (R,Z).

$$\psi(R,Z) = \frac{\Psi(R,Z)}{2\pi}, \text{ flux per radian}$$
$$\Psi(R,Z) = \iint d\vec{B}\cdot d\vec{S}$$

Current Flux

Poloidal current function, F, crossing the major circle, at (R,Z).

$$F(R,Z) = \mu I_{pol}\Psi(R,Z)/2\pi = R\,B_\phi$$
$$I_{pol}(R,Z) = \iint d\vec{j}_{pol}\cdot d\vec{S}$$

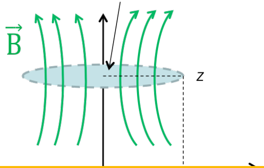

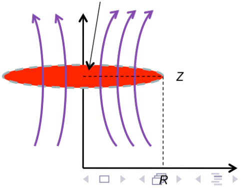

Axisymmetric Configuration

Equilibrium Flux Surfaces

Both Fluxes, (ψ, F) are constant on the `Flux Surfaces`:

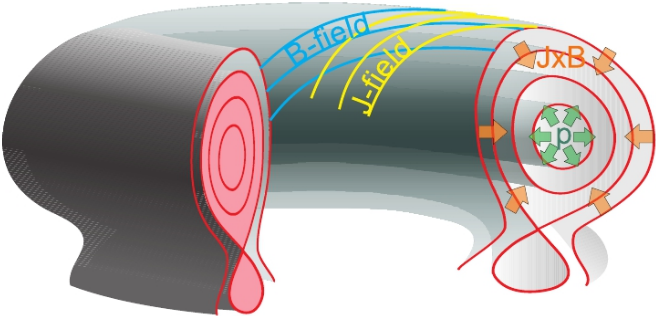

Toroidal Magnetic Field

Ampere's Law

$$\nabla \times \vec{B} = \vec{J_{free}}$$
$$\nabla F \times \hat{\phi} = \mu_0 R\, J_{pol} \text{ (poloidal comp.)}$$

- **In vacuum:** $\nabla F = 0$, so $B_\phi(R)$ varies only with $1/R$
  - Result: No information from the plasma taken from external local B_ϕ measurements

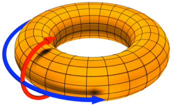

$$B_\phi = \frac{F}{R}$$

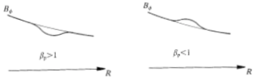

Diamagnetic Paramagnetic

Toroidal Magnetic Field

Ampere's Law

$$\begin{aligned} \nabla \times \vec{B} &= \vec{J_{free}} \\ \nabla F \times \hat{\phi} &= \mu_0 R\, J_{pol} \text{ (poloidal comp.)} \end{aligned}$$

- **In vacuum:** $\nabla F = 0$, so $B_\phi(R)$ varies only with $1/R$
    - Result: No information from the plasma taken from external local B_ϕ measurements

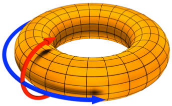

$$B_\phi = \frac{F}{R}$$

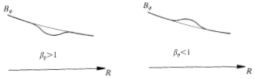

Diamagnetic Paramagnetic

Toroidal Magnetic Field

Ampere's Law

$$
\begin{aligned}
\nabla \times \vec{B} &= \vec{J_{free}} \\
\nabla F \times \hat{\phi} &= \mu_0 R\, J_{pol} \text{ (poloidal comp.)}
\end{aligned}
$$

- **Within Plasma:** $B_\phi(R, Z)$ depends on poloidal currents, J_{pol}.
  - **Diamagnetic loop** can measure the surface integral change.

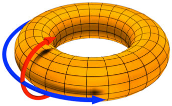

$$B_\phi = \frac{F}{R}$$

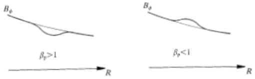

Diamagnetic Paramagnetic

Poloidal Magnetic Field

Ampere's Law (toroidal comp.)

$$\Delta^*\Psi \equiv R\frac{\partial}{\partial R}\left(\frac{1}{R}\frac{\partial\Psi}{\partial R}\right) + \frac{\partial^2\Psi}{\partial Z^2} = \mu_0 R J_\phi$$

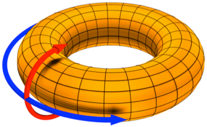

$$\begin{aligned}
\Psi(x') &= -\int_\Omega G(x,x')J_\phi(x)dx \\
&\quad + \oint_{\partial\Omega} \frac{1}{\mu_0 R}\left(\Psi\frac{\partial G}{\partial n} - G\frac{\partial\Psi}{\partial n}\right) dS \\
x' &= \text{point in } \Omega \\
G(x,x') &= \text{Green function for } \Delta^* \text{ operator.} \\
\frac{\partial}{\partial n} &= \text{normal derivative}
\end{aligned}$$

$$B_p = \frac{\nabla\Psi}{R}$$

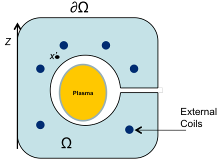

Equilibrium reconstruction

Basic restriction for external magnetic diagnostics

Green′s Theorem

Volume Domain Ω bounded by Plasma and $r \to \infty$.

$$\Psi(x') =$$

$$\boxed{-\int_{\Omega} G(x,x') J_{\phi}^{ext}(x) dx, \text{ Currents in external coils}}$$

$$+ \oint_{\partial\Omega} \frac{1}{\mu_0 R} \Psi \frac{\partial G}{\partial n} dS$$

$$- \oint_{\partial\Omega} \frac{1}{\mu_0 R} G \frac{\partial \Psi}{\partial n} dS$$

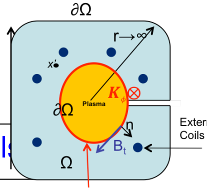

$$\Psi = C^{nst}$$

Equilibrium reconstruction

Basic restriction for external magnetic diagnostics

Green′s Theorem

Volume Domain Ω bounded by Plasma and $r \to \infty$.

$$\Psi(x') =$$
$$-\int_\Omega G(x,x')J_\phi^{ext}(x)dx$$
$$\boxed{+\oint_{\partial\Omega}\frac{1}{\mu_0 R}\Psi\frac{\partial G}{\partial n}dS\ ,\ \Psi = C^{nst}\text{ at the boundary}}$$
$$-\oint_{\partial\Omega}\frac{1}{\mu_0 R}G\frac{\partial\Psi}{\partial n}dS$$

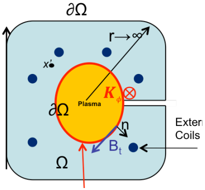

$\Psi = C^{nst}$

Equilibrium reconstruction

Basic restriction for external magnetic diagnostics

Green's Theorem

Volume Domain Ω bounded by Plasma and $r \to \infty$.

$$\Psi(x') = - \int_{\Omega} G(x,x') J_{\phi}(x) dx + \oint_{\partial\Omega} \frac{1}{\mu_0 R} \Psi \frac{\partial G}{\partial n} dS \boxed{- \oint_{\partial\Omega} \frac{1}{\mu_0 R} G \frac{\partial \Psi}{\partial n} dS}$$

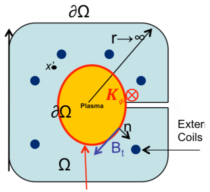

$\Psi = C^{nst}$

Term 3 is the only one that depends on internal current, J_{ϕ}^{plasma}.

Equilibrium reconstruction

Basic restriction for the magnetic diagnostics

BUT solution depends only on $B_t = \frac{1}{R}\frac{\partial \Psi}{\partial n}$ distribution on the Plasma boundary. There are infinitive distributions, $J_\phi^{plasma}(r)$, give the SAME B_t distribution.

Reconstruction $\Psi(R, Z)$ in Vacuum ☺

External measurements can determine the $\Psi(R, Z)$ anywhere in Ω and B_t on $\partial\Omega$. ☺

Reconstruction $\Psi(R, Z)$ inside Plasma ☹

External measurements alone CANNOT distinguish different internal current, $J_\phi(r)^{plasma}$ and $\Psi^{plasma}(R, Z)$ distributions INSIDE the plasma! ☹

Equilibrium reconstruction

Basic restriction for the magnetic diagnostics

BUT solution depends only on $B_t = \frac{1}{R}\frac{\partial\Psi}{\partial n}$ distribution on the Plasma boundary. There are infinitive distributions, $J_\phi^{plasma}(r)$, give the SAME B_t distribution.

Reconstruction $\Psi(R, Z)$ in Vacuum ☺

External measurements can determine the $\Psi(R, Z)$ anywhere in Ω and B_t on $\partial\Omega$. ☺

Reconstruction $\Psi(R, Z)$ inside Plasma ☹

External measurements alone CANNOT distinguish different internal current, $J_\phi(r)^{plasma}$ and $\Psi^{plasma}(R, Z)$ distributions INSIDE the plasma! ☹

ÉCNICO
ISBOA

Electrostatics Equivalent Parallel Case

The Electric Field outside the Sphere is the same for a given charge surface density or other (infinite) volume distributions.

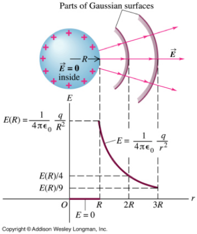

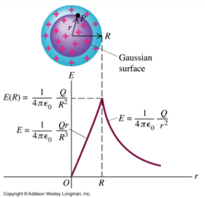

Reconstruction inside a sphere

External $\vec{E}(r)$ measurements CANNOT distinguish different Volume charge distributions.

Plasma Equilibrium in Fusion Plamas

Grad-Shafranov Equation

- Combining equation for Ψ with magnetic force balance $\nabla p = \vec{J} \times \vec{B}$ gives G-S equation inside the plasma:

$$\Delta^{*}\Psi = -\mu_0 R\, J_{\phi} = -\mu_0 R^2 \frac{dp}{d\Psi} - \frac{1}{2}\frac{dF^2}{d\Psi}$$

- G-S gives additional constraint on $\vec{B}$ within the plasma but also introduces another unknown scalar functions: the pressure and current
- Need to make some assumptions on $p(\Psi)$ and $F(\Psi)$ to calculate full plasma equilibrium solution.

Plasma Equilibrium
Example: JET Reconstruction

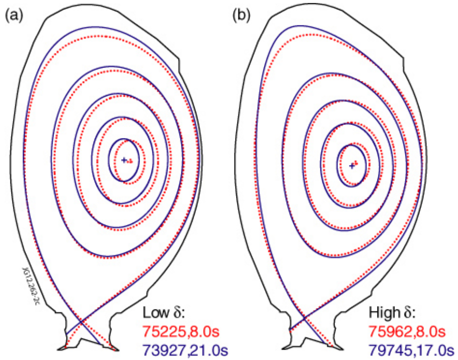

Magnetic configuration of the (a) low- and (b) high-triangularity plasmas for the hybrid (red) and baseline H-mode (blue) plasmas.

Magnetic Inductive Sensors

Basic Types

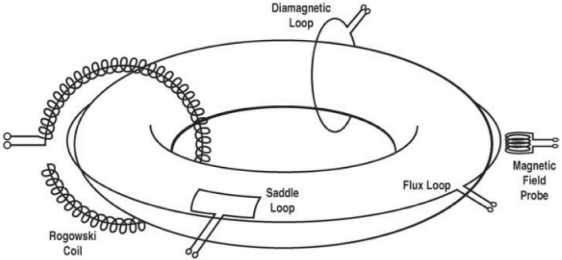

Schematic figure of a toroidal plasma, showing the basic types of inductive sensors.

Magnetic Inductive Sensors

Probe signal is always a time derivative

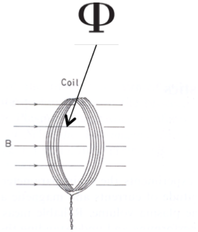

Mag. Flux on the Sensor Loops

$$\begin{aligned} V_{sensor}(t) &= \oint \vec{E} \cdot \vec{ds} = -\frac{\partial \Phi(t)}{\partial t} = NA\dot{B} \text{ (Faraday Law)} \\ \Phi(t) &= \int_{t_0}^{t} V_{sensor}(t')dt' \\ B &\cong -\frac{\Phi(t)}{NA} = -\frac{\int_{t_0}^{t} V_{sensor}(t')dt'}{NA}, \text{ (A: Loop Area)} \end{aligned}$$

Magnetic Inductive Sensors

Rogowski Coil

- Measures total electric current flowing through the enclosed surface,
    - e.g. plasma, plasma + vessel, external coils, passive conductors, Halo Currents, etc.
- If $|\Delta B|/B \ll n$ (n is turns / m), total flux is:
  $\Phi = n \oint_{\ell} \int_{A} \vec{B} \cdot \vec{d\ell} dA = nA\mu_0 I_p$
- Signal is proportional to current time derivative:
  $V(t) = \dot{\Phi} = nA\mu_0 \dot{I}_p$

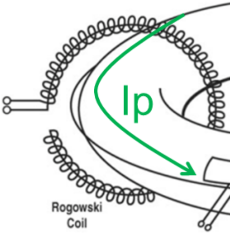

Conducting path from one end must return along the axis to the other end

Magnetic Inductive Sensors

Sinus-cosinus Coil

- A variation of Rogowski Coil but winding density, $n(\theta)$, varies with $\sin(\theta)$ or $\cos(\theta)$
- Used to measure Plasma Displacements

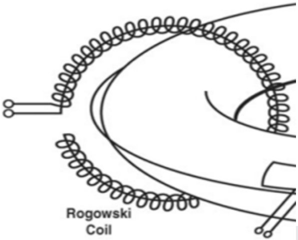

Magnetic Inductive Sensors

Poloidal Flux Loops

- Measures $\Psi(R,Z)$ on a given (R,Z)
- On Iron Core Tokamaks with ohmic heating, most of the poloidal flux is on the core itself: $B = \mu_r \mu_0 H$, $\mu_r(iron) \approx 4000$
- To improve the sensivity, a smaller loop is chosen as reference and subtracted from others: $\Psi_i = \Psi(R,Z) - \Psi_{ref}$

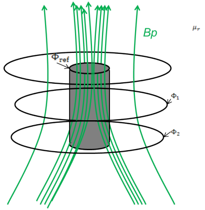

Loop Voltage

Voltage signal from a flux loop is the local one-turn V_{loop}, which drives I_p

Magnetic Inductive Sensors

Diamagnetic Loop

- Measures the toroidal magnetic flux for the purpose of estimating the thermal energy of the plasma $\langle p \rangle \propto W$.
- Normally located in a poloidal plane to minimize coupling to the B_{pol}.
- At low beta, the change in the total toroidal flux is small. $\beta = 2\mu_0 \langle p \rangle / B^2 \ll 1$

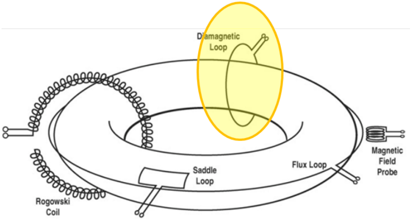

A reference signal coupled to $B_{\phi,vacuum}$ is usually subtracted: $\Delta\Phi_{Diag} = \Phi_{total} - \Phi_{vacuum}$

Basic Magnetic Inductive Sensors

Integral quantities

- Total **Plasma Current** , I_ϕ (Rogow.)
- **Ohmic Power** (Rogow+ V. Loop)

$$P \equiv \int_{Vol} \vec{E} \cdot \vec{j} \, d^3x = V_\phi I_\phi - \frac{\partial}{\partial t}(\frac{1}{2} L I_\phi^2)$$

- **Poloidal beta** , β_p, (Rogow+ Diag. Lop)
  $\beta_p \equiv 2\mu_0 \langle p \rangle / B_{p,a}^2 (\ll 1)$, $B_{p,a} = \mu_0 \, I_\phi / \Gamma$, Γ is length of a poloidal plasma contour.
  - Circular Plasma $\beta_p = 1 - \frac{8\pi B_{\phi,vacuum}}{(\mu_0 I_\phi)^2} \Delta\Phi_{Diag}$
  - Non-Circular Plasma

$$\beta_p \approx 1 - \frac{1+\kappa^2}{2\kappa} \frac{8\pi B_{\phi,vacuum}}{(\mu_0 I_\phi)^2} \Delta\Phi_{Diag}$$

κ is the vertical elongation of plasma

Basic Magnetic Inductive Sensors

Integral quantities II

- Total **Shafranov shift** , Δ. (From Rogow. + Vertical Field Current)

At Large Aspect Ration approximation:

$$\Delta' = \frac{r}{R}\Lambda, \quad \Lambda = \beta_{pol} + \ell_i/2$$

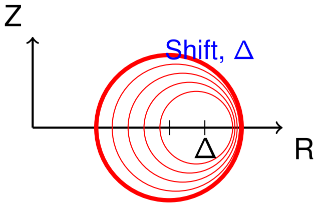

Basic Magnetic Inductive Sensors

Integral quantities III

- **Plasma conductivity** , σ (Rogow+ V. Loop)

$$\hat{\sigma} = \frac{2\pi R}{\pi a^2} \frac{I_\phi^2}{P}, (\text{ if } \frac{\partial}{\partial t} = 0)$$

- **Electron Temperature** , T_e

$$\sigma = 1.9 \times 10^4 \left(\frac{T_e^{3/2}}{Z_\sigma \ln \Lambda} \right)$$

  - Z_σ, resistance anomaly determined by ion charge
  - $\ln \Lambda$, Coulomb logarithm:

$$\ln \Lambda \approx 31 - \ln(n_e^{1/2} / T_e)$$

Magnetic Inductive Sensors

Plasma Displacement

- Cylindrical Approximation $R \gg a$. Plasma Displaced by $\Delta \ll a$

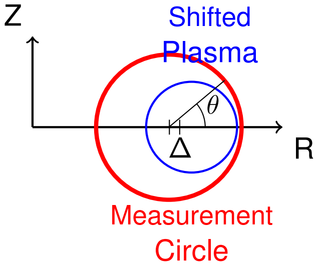

- Measured poloidal field is:

$$
\begin{aligned}
B_\theta(\theta) &= \frac{\mu_0 I}{2\pi a} \frac{1}{\left[\sin^2\theta + (\cos\theta - \Delta/a)^2\right]^{1/2}} \\
&= \frac{\mu_0 I}{2\pi a} \left(1 + \frac{\Delta}{a}\cos\theta\right)
\end{aligned}
$$

- Displacement can extracted from the Sinus-cosinus Coils.

Magnetic Local Probes

- Probes measure components of the local magnetic field strength.
- Usually solenoidal, with dimensions small compared to the gradient scale length of the magnetic field.

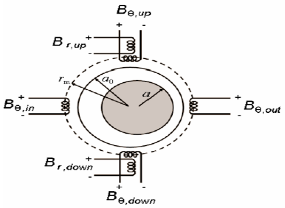

$$\Phi_{probe} = N\,A\,B_{\|}$$

Magnetic Local Probes

Shielding

- Probes should be located on the plasma-facing side of the vacuum vessel wall.
- Should be oriented to measure the field tangential to the wall; otherwise, eddy currents in the wall will attenuate the high-frequency part of the signal.

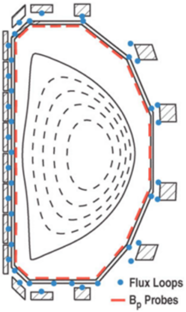

Magnetic Local Probes

Shielding

- Shielding of the tangential field by the conductive wall.

$$\frac{B(inside)}{B_0} = \frac{1+2i\omega\tau_w}{1+i\omega\tau_w}$$

$$\frac{B(outside)}{B_0} = \frac{1}{1+i\omega\tau_w}$$

τ_w is the characteristic time for the magnetic flux to diffuse through the wall

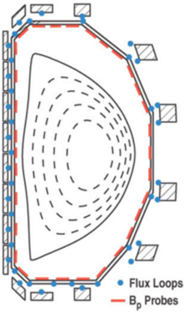

Saddle Loops

Can be viewed as

- A large-scale magnetic probe for the magnetic field normal to the surface. $\Phi(saddle) = N\,A\langle B_\perp\rangle$
- or as probes measuring Flux Difference: .
  $\Phi(saddle) = N\,\Delta_\phi\,\Delta_\psi$

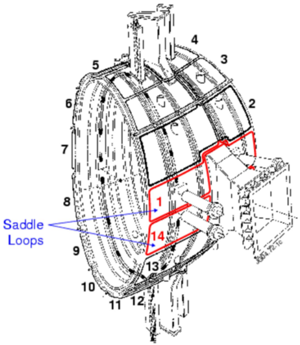

Determination of Plasma Shape

1. Taking measurements of the $\Psi(R, Z)$ and poloidal B_{pol} near the Wall, plus the currents in external Coils allows local Ψ extrapolation.
2. Plot the contours of $\Psi(R, Z) = C^{nst}$. Find the Last Closed Flux Surface LCFS, or Separatrix in Divertor tokamaks

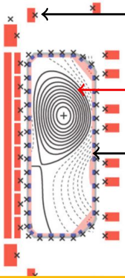

Flux Loops $\Psi(R, Z)$

LCFS

Magnetic Probes $B(R, Z)$

Separatrix

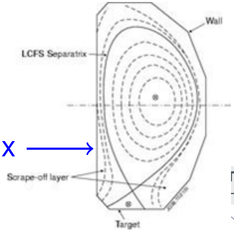

Determination of Plasma Shape

1. Taking measurements of the $\Psi(R, Z)$ and poloidal B_{pol} near the Wall, plus the currents in external Coils allows local Ψ extrapolation.
2. Plot the contours of $\Psi(R, Z) = C^{nst}$. Find the Last Closed Flux Surface LCFS, or Separatrix in Divertor tokamaks

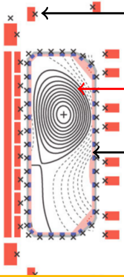

Flux Loops $\Psi(R, Z)$

LCFS

Magnetic Probes $B(R, Z)$

Separatrix

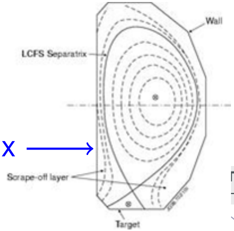

Outline

Integration of signals from Mag. Sensors

Analog Integration

- To obtain the fluxes and magnetic field values from inductive sensors we must integrate the signal in time: $V_{out}(t) = -\frac{1}{\tau}\int_0^t V_{in}(t')dt' = \Phi(t)/\tau$

- Typical loop flux values vary from few $mV.s$ to $V.s$ (e.g. Iron core), so integrator circuits are used with $1\ ms < \tau < 1\ s$.

Integration of signals

Analog Passive Integrator

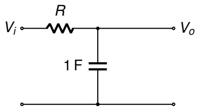

- Simple Passive Integrator (RC Low Pass Filter, 1^{rst} Order , $-20dB/dec.$), $\tau = RC$

$$V_{out}(\omega) = -\frac{1}{1 + i\omega\tau} V_{in}(\omega) \Rightarrow V_{out}(t) \approx -\frac{1}{\tau}\int_{t_0}^{t} V_{in}(t')dt'$$

RC Limitation!

The approximation fails for timescales $t \geq RC$.

Integration of signals
Analog Active (Op-Amp) Integrator

- Gain is similar to passive integrator, $1/RC$, but timescale is increased from $\sim RC \rightarrow \sim G \cdot RC$ (1 ms to 10 s).

NEW problem: Integrator Drift by OpAmp Input V_{off}

Example: for $RC = 10\,ms$ a $V_{off} = 100\,\mu V$ integrates to a $0.1\,V$ after $10s$

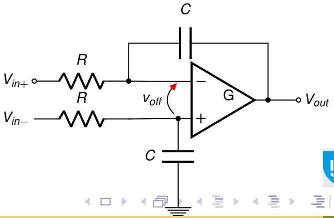

Integration of signals

Analog Active (Op-Amp) Integrator

- Gain is similar to passive integrator, $1/RC$, but timescale is increased from $\sim RC \rightarrow \sim G \cdot RC$ (1 *ms* to 10 *s*).

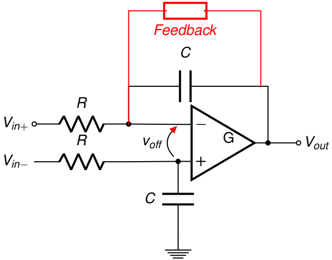

Solution

Basic compensation circuit

Analog Integrators
Advanced Designs

- Automatic drift-compensation: Measurement of drift before integration, store and compensate offset during integration.
- Drift can be reduced down to $1 mVs@1000s$
- But worse values if signal is applied during drift compensation!

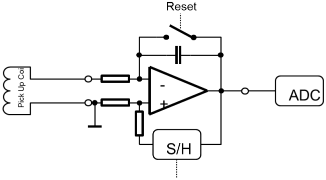

Analog Integrators

Advanced Designs

- Automatic drift-compensation: Measurement of drift before integration, store and compensate offset during integration.
- Drift can be reduced down to $1mVs@1000s$
- But worse values if signal is applied during drift compensation!

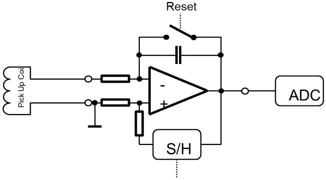

Analog Integrators
Advanced Designs

- Automatic drift-compensation: Measurement of drift before integration, store and compensate offset during integration.
- Drift can be reduced down to $1mVs@1000s$
- But worse values if signal is applied during drift compensation!

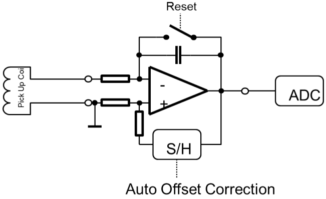

Digital Integrators

Chopper Input

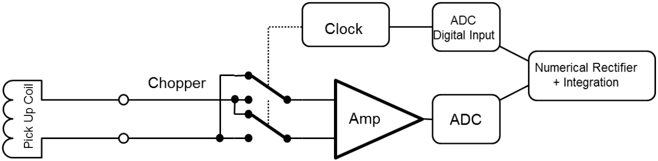

- Dynamic range limited by input stage
- Not affected by input stage semiconductors
- Offset correction algorithms feasible in Real Time (e.g. FPGA)

Digital Integrators

W7-X / IST ADC chopper module

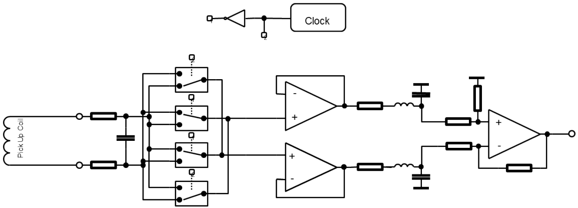

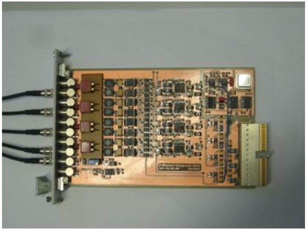

Digital Integrators

IST prototype

- 100s Drift measuring compensation phase
- Drift Compensated in FPGA
- Drift reduced down to $< 500\mu V \cdot s@1000s$

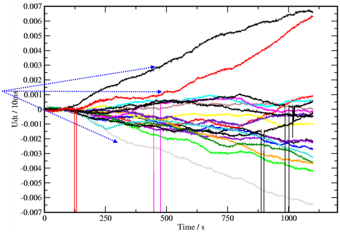

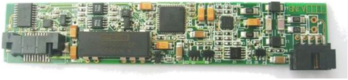

IST/F4E prototype for chopper digital integrator

ITER magnetics

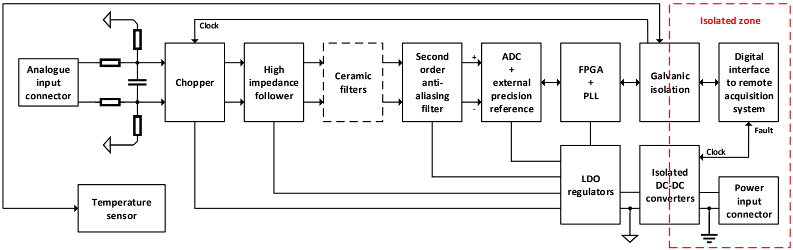

Outline

Diagnostics using non-Integrated Signal

Inductive probes

- Direct information on Plasma Speed: $V(t) \propto I_{plasma}(t) \cdot Vel_{R,Z}(t)$
  - Used as controllable variables for active control
- Usually as linear combinations of flux loops and field probes (analog electronic adders)

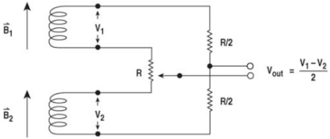

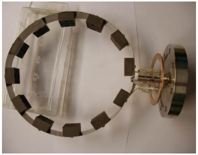

Diagnostics using non-Integrated Signal

Inductive probes

- High Frequency MHD plasma instabilities detection and control
  $V(t) \propto \dot{B}(t) \sim \omega B(t)$
  - Mirnov coils, poloidal or toroidal arrays oriented to measure $\dot{B}_{pol}(t)$

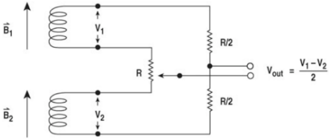

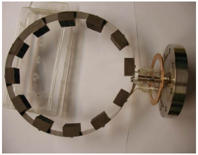

Non-Integrated Signal
MHD Instabilities Diagnostics

- Analyses Techniques: Spectrogram (Fourier analysis of successive short-time windows).
- Other techniques:
  - Wavelet analysis.
  - Hilbert transform.
  - Singular Value Decomposition (SVD).

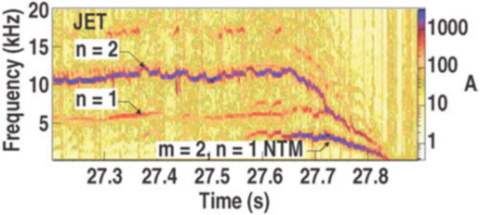

Non-Integrated Signal

MHD Instabilities mode number detection

- Usual MHD perturbation: $\delta B(t) \propto \delta B(r) \cos(m\theta + n\phi - \omega t)$
- Mode numbers m, n can be determined by the phase shift between equally separated Mirnov coils, by Fourier Analysis.

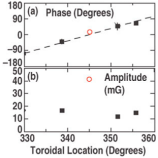

Identification of the toroidal mode number $n = 7$ of a compressional Alfven eigenmode in NSTX.

Non-Integrated Signal

Auto and Cross Correlation between two signals

Defining a dot product between 2 functions

$$< f, g >= \int_{-\infty}^{\infty} f^*(t)g(t)dt$$

Cross-correlation :

$$\begin{cases} (f * g)(\tau) = \int_{-\infty}^{\infty} f^*(t)f(t+\tau)dt & \text{Continuous,} \\ (f * g)[n] = \sum_{m=-\infty}^{\infty} f^*[n]g[n+m] & \text{Discrete.} \end{cases}$$

Auto-correlation :

$$\begin{cases} (f * f)(\tau) = \int_{-\infty}^{\infty} f^*(t)f(t+\tau)dt & \text{Continuous,} \\ (f * f)[n] = \sum_{m=-\infty}^{\infty} f^*[n]f[n+m] & \text{Discrete.} \end{cases}$$

Non-Integrated Signal

Auto and Cross Correlation between two signals

Cross-correlation of real life finite sampled signals

- Real life signals have only limited number of samples
- Cross-correlation easier to interpret when bounded in [-1,1]
- Lag vector (index-n) also finite
- MATLAB/Octave Funtion *r= xcorr(x , y)*

$$(f * g)[n] = \begin{cases} \dfrac{\sum_{m=1}^{N-|n|} (f[m+|n|]-\bar{f})(g[n]-\bar{g})}{\sqrt{\sum_{m=1}^{N} (f[m]-\bar{f})^2} \sqrt{\sum_{m=1}^{N} (g[m]-\bar{g})^2}} & \text{if } n < 0, \\ \\ \dfrac{\sum_{m=1}^{N-n} (f[m]-\bar{f})(g[n+m]-\bar{g})}{\sqrt{\sum_{m=1}^{N} (f[m]-\bar{f})^2} \sqrt{\sum_{m=1}^{N} (g[m]-\bar{g})^2}} & \text{if } n \geq 0. \end{cases}$$

Non-Integrated Signal

Cross Correlation as wavenumber *m, n* estimator

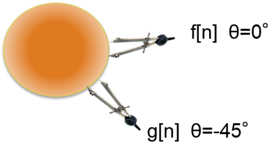

$$
\begin{aligned}
f[n] &= \cos(w_1 t[n] - k\theta_1)\\
g[n] &= \cos(w_1 t[n] - k\theta_2)
\end{aligned}
$$

$$
\begin{aligned}
w_1 t[n + lag_{max}] - k\theta_2 &= w_1 t[n] - k\theta_1\\
w_1(t[n + lag_{max}] - t[n]) &= k(\theta_2 - \theta_1)\\
k &= \frac{w_1 \cdot t[lag_{max}]}{\theta_2 - \theta_1}
\end{aligned}
$$

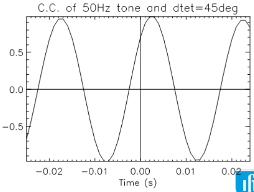

Non-Integrated Signal

$\theta - t$ space visual analysis

Example

- Magnetic coils :$i = 1 \ldots 12$ eq. spaced in poloidal plane
- $s_i(t) = \cos(\pi f t + m\theta_i) + noise(\mu = 0, \sigma = 0.2)$

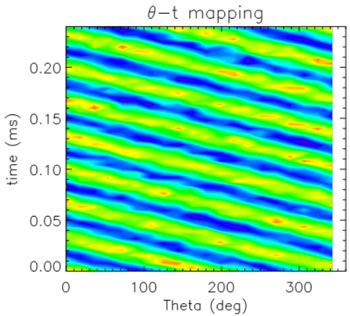

- Wave front propagates clockwise
- Two periods for fixed t (m=2)
- Period $\approx$ $0.03ms$ f $30kHz$

Non-Integrated Signal
MHD Nonrotating Modes

- Nonrotating modes are most commonly detected with toroidal arrays of **saddle coils**
- At low frequencies involved the field perturbation penetrates the vacuum vessel.

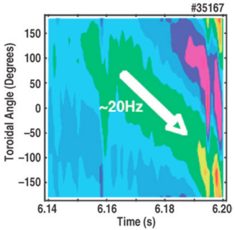

Time evolution of an RWM in JT-60U measured with an array of eight saddle coils.

Outline

Non Inductive Sensors

- Signal has direct Value: $v(t) \propto B(t)$.
- Hall Probes are relatively simple and inexpensive. $V_H = \frac{1}{qn}\frac{I_H B}{a}$, $\frac{1}{qn}$ is **Hall coefficient**, is a property of each material.
- low frequency, low sensivity, very sensible to radiation!

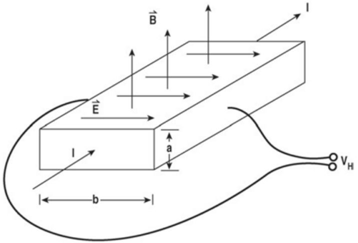

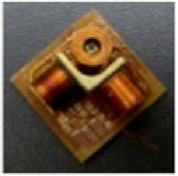

Non Inductive Sensors II

- Resistive Shunts:
  - Measuring halo currents flowing between the plasma and plasma-facing components
- Faraday rotation current measurements:

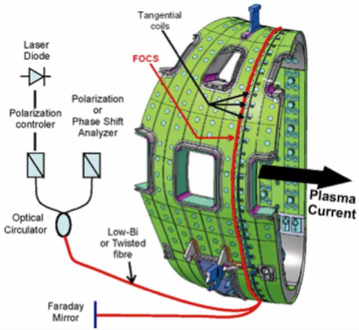

Schematic overview of a fiber-optic Faraday rotation measurement device.

Non Inductive Sensors III

Faraday effect

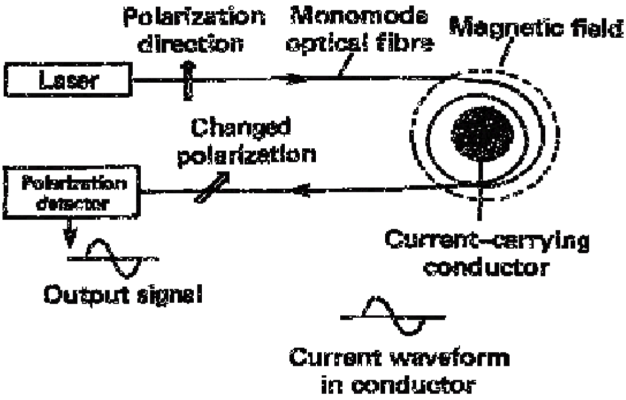

Scheme of the Faraday effect measurement.

Non Inductive Sensors IV

Fluxgate Magnetometer

Basic sensor configuration.

- The core is excited by an AC current I_{exc}.
- The signal induced in the sense coil V_{ind} at the second harmonic of I_{exc} proportional to the external field B_o.

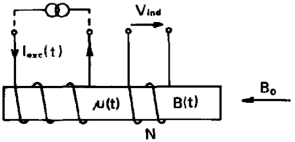

Fluxgate Magnetometer.

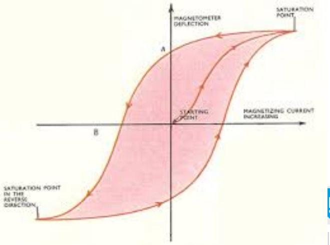

Non Inductive Sensors IV

Fluxgate Magnetometer

- Capable of measuring low frequency DC/ AC fields in the range $10^{-10} - 10^{-4}T$
- The signal induced in the sense coil V_{ind} at the second harmonic of I_{exc} proportional to the external field B_o.
- Usually double core is adopted

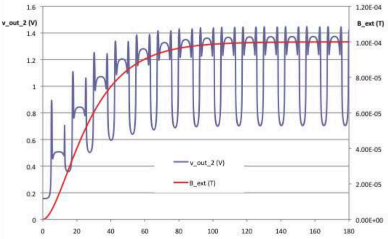

Waveform of sensor signal with variable external magnetic (Red curve .

Non Inductive Sensors V

MEMS magnetic field sensors

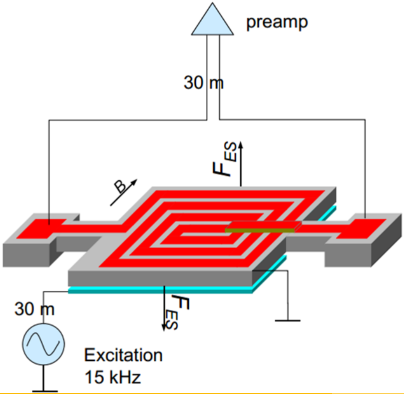

Outline

Burning plasma experiments
ITER

- ITER will be the first burning plasma experiment
- Relative to existing machines (e.g. JET), ITER diagnostic components will be subjected to:
  - High *n* and γ fluxes.
  - *n* Heating (now essentially zero).
  - High fluxes of energetic neutral particles.
  - Long pulse lengths.

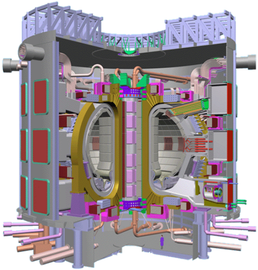

ITER diagnostics

Magnetic Set

Total $\tilde{1}700$ sensors, 19 types, $>$ 300 *km* of cable

Location	Radiation/Dose (cm^{-2} s^{-1}) / MGy		Type	Number
	n	γ		
In-vessel sensors: Behind blanket modules, fixed on VV inner skin	3. 10^{12} 500	1. 10^{12} 340	Pick-up coils	186
			Rogowski (halo current)	360
			Flux loops	220
	1. 10^{13} 1700	3. 10^{12} 1000	High freq coils	>300
Divertor	1. 10^{13} 1700	3. 10^{12} 1000	Pick-up coils	72
			Rogowski (halo current)	48
Ex-vessel sensors Fixed on VV outer skin	1.5 10^{10} 2.5	1. 10^{10} 3.4	Pick-up coils	360
			Steady state sensors	120
			Flux loops	5
			Optic fibre	12
Inside TFC case (T=4K)	1. 10^{10} 1.7	2. 10^{9} 0.7	Rogowski (I plasma)	≥ 3

ITER diagnostics

Poloidal Magnetic Set

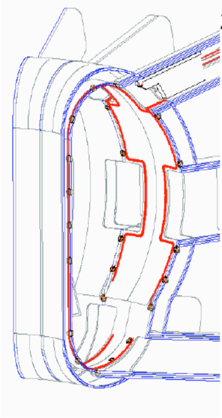

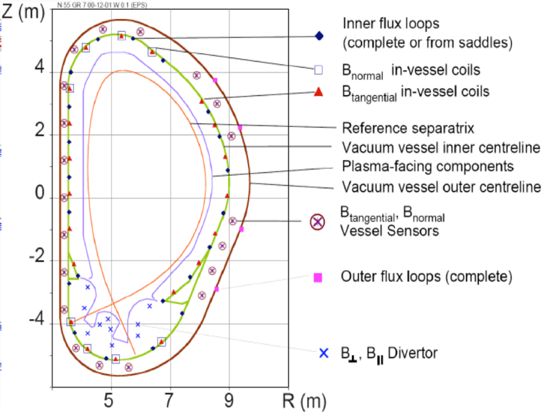

Structure of Magnetosphere
Earth Fields

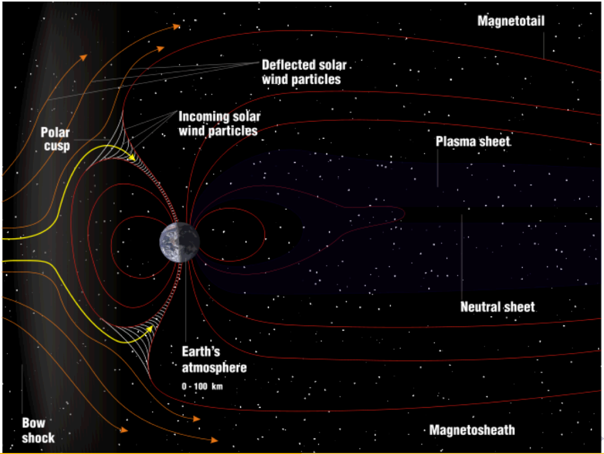

Magnetosphere

Plasma Diagnostic

Further Reading I

I. H. Hutchinson
Principles of Plasma Diagnostics.
Cambridge University Press, 2005.

E. J. Strait et al.
Plasma Diagnostics for Magnetic Fusion Research, ch. 2.
Fusion Science and Technology, special Issue ,Vol. 53, No. 2, February 2008

A. Wootton
Magnetic Fields and Magnetic Diagnostics for Tokamak Plasmas, 2008, `web2.ph.utexas.edu/~iheds/magneticfieldsinatokamak.pdf`